Stable, three layered organic memory devices from C_{60} molecules and insulating polymers

Alokik Kanwal and Manish Chhowalla[a)]
Materials Science and Engineering, Rutgers University, 607 Taylor Road, Piscataway, New Jersey 08854

(Received 30 August 2006; accepted 5 October 2006; published online 14 November 2006)

Memory devices based on C_{60} fullerene molecules and polystyrene and poly 4-vinyl phenol polymers are described. It is shown that the bistability in the $I-V$ characteristics can be used to perform read-write-erase memory functions. In addition, it is demonstrated that mild thermal annealing enhances the stability of the devices. Specifically, after annealing, the hysteresis in our devices can be preserved up to 85 °C in 60% humidity. Furthermore, memory retention tests show that it is possible to preserve a state even after annealing at 85 °C in 60% humidity for 30 min. © *2006 American Institute of Physics*. [DOI: 10.1063/1.2388131]

Memory devices play an important role in electronics, accounting for more than 20% of the semiconductor market.[1] Most memories are fabricated using the complimentary metal oxide semiconductor technology. Memory devices from organic materials have recently begun to receive attention.[2–13] Although there is a clear demand for next generation of nonvolatile solid state memories, the newcomer organic memory devices must exceed the existing speed and cost constraints of today's entrenched technologies.[3] In addition, the new technology must also meet other critical performance criteria such as long term data retention, low power consumption, and large number of rewrite cycles.[3]

Numerous organic materials have been proposed for devices such as field effect transistors, light emitting diodes, and solar cells.[14–20] In contrast, few reports on organic memory devices have appeared only recently.[2–13] Most of the reported organic memory devices are, in fact, hybrids of inorganic nanoparticles dispersed in a polymer which is then sandwiched between two metal electrodes.[2–10] The current-voltage characteristics of these hybrid memory devices generally exhibit bistability which is used as the basis for the memory device.[2–11]

Memory effect in organic materials fabricated using C_{60} fullerene molecules dispersed in an insulating polymer has also been recently reported.[12,13,21] The memory effect was measured by sandwiching the polymer/C_{60} layer between two Al electrodes. It was demonstrated that the hysteresis in the $I-V$ sweep was due to charge storage and retention in C_{60} molecules at room temperature. Unfortunately, the current values between the high and low conducting states were low (~100 nA), making it difficult to distinguish between the two. Furthermore, similar to other the literature,[2–11] information regarding the stability of the polymer/C_{60} memory devices was not reported.[12,13,21]

In this letter, we demonstrate that it is possible to improve the difference between high (few microamperes) and low (less than 1 pA) conduction states in our C_{60}/insulating polymer memory devices by adopting a three layer device structure. The structure is unique because it incorporates a thin buffer polymer between the bottom electrode and the polymer/C_{60} (also referred to as nanocomposite throughout this letter) layer and a thick capping layer between the nanocomposite layer and the top electrode. In addition, we describe a method of mild thermal annealing which in turn enhances the stability of the devices. Specifically, after annealing, the hysteresis in our devices can be preserved up to 85° C in 60% humidity. Furthermore, memory retention tests show that it is possible to preserve a state even after annealing at 85° C in 60% humidity for 24 min.

The three layer memory devices were fabricated in the cross point architecture as shown in Fig. 1(a). The electrode width and thickness were 0.5 mm and 90 nm, respectively. The cross sectional view of the three layer devices is shown schematically in Fig. 1(a) (ii). Initially, the bottom electrode Al strips were thermally evaporated through a shadow mask at a base pressure of 1×10^{-6} Torr onto clean glass substrates. Subsequent to Al evaporation, a very thin layer (<3 nm) of polystyrene (PS) polymer was spin coated from solution onto the substrate. The very thin films were achieved by deposition at high spin coating speeds (7500 rpm) and using a dilute solution (less than 10 mg of PS in 1 ml of toluene). Measurement of the exact thickness of this very thin layer was difficult but its role in preventing shorting between the nanocomposite layer and the bottom electrodes was found to be essential. Repeatability in terms of the device performance in the absence of this very thin

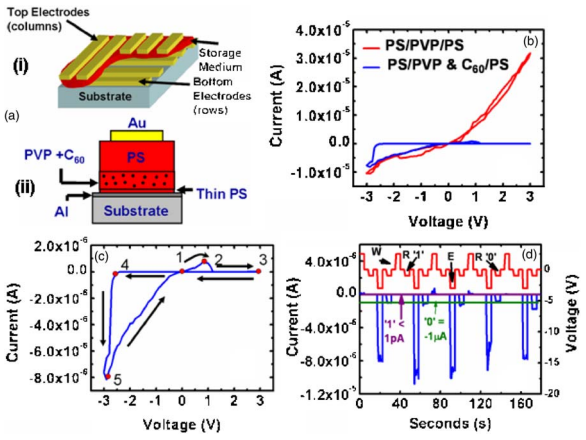

FIG. 1. (Color online) (a) Schematic of the (i) cross point architecture (adapted from Ref. 3) and (ii) cross sectional view of the three layer memory devices. (b) I-V characteristics of Al/PS/PVP/PS/Au and Al/PS/PVP+C_{60}/PS/Au devices. In the absence of C_{60} molecules, no hysteresis is observed. (c) Enlargement of the hysteresis observed in Al/PS/PVP+C_{60}/PS/Au devices. (d) Demonstration of programmability of read-write-erase functions. Write voltage=+2.5 V, read voltage=−1 V for both 0 and 1 states, and erase voltage=−3 V.

a)Electronic mail: manish1@rci.rutgers.edu

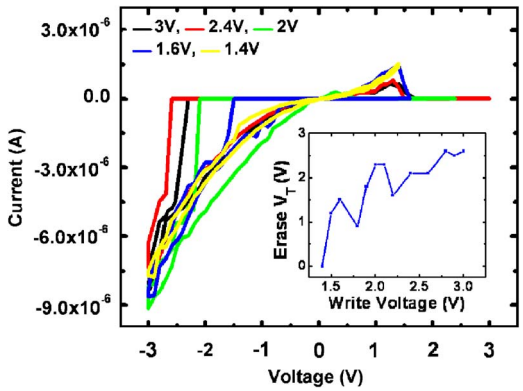

FIG. 2. (Color online) The Variation of discharge voltage with maximum positive voltage applied. The listed voltages are the maximum positive voltages applied. No hysteresis is observed when the maximum applied positive voltage is +1.4, indicating that most C_{60} molecules are not charged. The inset shows the variation of the erase threshold voltage (V_T) with maximum write voltage.

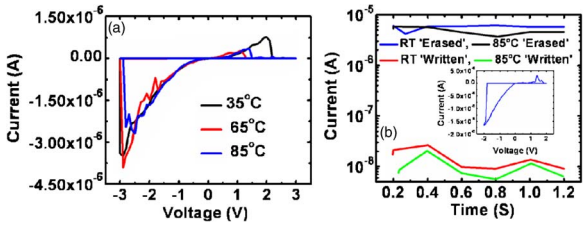

FIG. 3. (Color online) Demonstration of stability and retention in our memory devices. (a) Measurement of the hysteresis at three different temperatures in 60% humidity. (b) This graph shows that the device remains in the same state (either written or erased state at room temperature) after annealing in 60% humidity at 85 °C.

layer was found to be poor. After the deposition of the thin barrier, ~20 nm thick layer of the poly 4-vinyl phenol (PVP)+C_{60} nancomposite was spin coated (7400 rpm) on top. The concentration of C_{60}, PVP, and solvent was 0.5 mg of C_{60} in 25 mg of PVP in 1 ml of isopropyl alcohol (concentration of C_{60} in solution is 5% by weight). Our calculations and measurements indicate that the percolation threshold of C_{60} in PVP is ~18%. Therefore at 5%. we expect the C_{60} molecules to be completely isolated from each other as long as they are fully dissolved in the solution. Finally, the PS capping layer (thickness ~30 nm) was deposited by dissolving 10 mg of PS in 1 ml of toluene and spin coating the solution at 7000 rpm. After the deposition of the three layers, the substrates were replaced in the thermal evaporator and gold electrodes (90 nm thick and 0.5 mm wide) perpendicular to the bottom electrodes were deposited, completing the cross point architecture. The electrical measurements on the memory devices were made using an Agilent 4156C semiconductor analyzer at room temperature with a sweep rate of 10 ms/V.

The current–voltage ($I-V$) characteristics from the three layer cross point devices are shown in Fig. 1(b). The bottom electrode was grounded and voltage on the top electrode is swept from +3 to −3 V. Two types of devices were measured in order to investigate the role of C_{60} molecules in charge storage. In the reference device, the three layers were deposited as described above but in the second layer, pure PVP without the C_{60} molecules was deposited. Typical I-V characteristics from the reference devices are shown in Fig. 1(b) where it can be clearly observed that in the absence of C_{60} molecules, no hysteresis is found. In contrast, for the device with the PVP+C_{60} nanocomposite layer, a distinct hysteresis at negative voltages can be observed. It can also be observed that the current increases at positive voltages for the polymer only devices, in contrast to the devices containing C_{60} molecules. Our analysis of the measured data indicates that the charge injection from the Al electrode into the polymer can be described by direct tunneling at low fields and by Fowler-Nordheim tunneling at high fields, consistent with the literature.[22] The transport through the polymer is via hopping, as determined by fitting the data (not shown). It should be mentioned that in the polymer only devices, a hysteresis can be measured initially but disappears after the two to three sweeps. This is attributed to the presence of electronegative OH molecules in the benzene rings of the PVP which act as traps for electrons. However, in contrast to C_{60}, the OH molecules are relatively unstable and not as electronegative so that repeatable charge storage and discharge is not possible.

In order to demonstrate the hysteresis more clearly, it is replotted in Fig. 1(c). The appearance of the hysteresis can be described in the following manner. Initially, in the off state at point 1 in Fig. 1(c), the measured current value is less than 1 pA (the sensitivity of our measurement unit). As the voltage is increased, electrons are injected from the bottom Al contact into the nanocomposite layer via tunneling through the very thin insulating layer and the measured current increases. Some of the electrons are injected into the C_{60} molecules where they are essentially trapped due to the high electronegativitiy of fullerenes. As sufficiently large amounts of electrons are trapped by the C_{60} molecules, the current through the sandwich structure begins to decrease as indicated by point 2 in Fig. 1(c). The decrease in the current at point 2 is attributed to the screening of the applied electric field due to storage of charge in the nanocomposite layer. As the voltage is further increased up to +3 V, more isolated C_{60} molecules become charged which increases the screening so that the device remains in the low conduction state, as indicated by point 3. In contrast, the absence of charging and therefore screening in the polymer only devices leads to an increase in current at high positive voltages. As the voltage is decreased, the device remains in the low conduction state until a critical voltage (<−2.5 V) is reached where the C_{60} molecules are discharged, point 4 in Fig. 1(c). The discharge of trapped carriers leads to a large increase in current and the device goes into a high conduction state mode, point 5. Once the device is fully discharged, increasing the voltage leads to a steady decrease in current which follows a different path back towards point 1, as indicated by the arrow in Fig. 1(c), giving rise to a hysteresis.

In order to translate the hysteresis into memory device operations, read-write-erase functions were performed. The behavior of a device during the programming of the various states is plotted in Fig. 1(d). Relatively slow voltage pulses of 4 ms were used to program the different functions. A voltage of −1 V was chosen to read the "0" or "1" states. At this voltage, the difference between the on and off states (on/off ratio) is greater than 10^7, making them easily distinguishable. More importantly, the read current is microamperes which allows it to be read without requiring additional amplification. Initially, a +2.5 V pulse is applied in order to write the 1 state. After the voltage pulse, the device is disconnected for 5 s when a read pulse of −1 V is applied. It can be seen from Fig. 1(d) that the device after the read step remains in the

low conduction state. In order to erase the charge from the write step, a −3 V pulse is applied which switches the device into the high conduction state. The erasure of the device is confirmed by applying a voltage pulse of −1 V which shows that the device is in the high conduction state (0 state) with a current value of $\sim 1(\pm 0.5)$ μA, as shown in Fig. 1(d). The characteristics in Fig. 1(d) indicate that the device is programmable at long time scales. However, in order to demonstrate that the devices can switch at high speeds, we also performed nanoscale measurements. In agreement with our previous results, we find switching time of the order of 10 ns, indicating that fast switching is possible in these devices.[12,13]

Since the charging of the C_{60} molecules is determined by the maximum positive voltage applied, it should be possible to vary the characteristics of the observed hysteresis because the discharge voltage depends on the amount of screening. This is useful in memory devices for writing multiple bits per cell. The variation of the hysteresis as a function the maximum positive voltage applied is shown in Fig. 2. It can be seen from the figure that for maximum positive voltages above +1.6 V, hysteresis in the *I-V* characteristics can be observed. Furthermore, the discharge voltage (see inset) also depends on the maximum positive voltage applied. At a maximum applied voltage of +1.4 V, no hysteresis is observed. It is interesting to note that the overall current through the device in all the measurements is similar, indicating that carrier injection and transport through the polymer are unaffected. If, however, the number of carriers injected into the polymer is the same, then the amount charged C_{60} molecules should be same in all measurements. This is clearly not what is observed in Fig. 2. The fact that the C_{60} molecules are not charged at +1.4 V indicates that there is an energy barrier (β) between the PVP polymer and the fullerenes which is between $1.4\ \text{eV} < \beta < 1.6\ \text{eV}$.

Finally, we discuss the stability of our devices, an issue with all organic devices. In addition to concerns about environmental stability, there is also a question whether the devices can operate at temperatures near the glass transition temperature of PS ($\sim 100\ ^\circ\text{C}$). Initially, we investigated the stability of our as fabricated devices and found that they degraded rapidly with temperature. However, we discovered that after thermal annealing at 50 °C for 5 min in vacuum, the stability of our devices increased dramatically. The *I-V* curves measured at three different temperatures in 60% humidity are shown in Fig. 3(a). It can be seen that the hysteresis is preserved up to 85 °C. The enhanced stability of the devices is attributed to the increase in cross-linking of the polymers after annealing. However, the annealing must be closely controlled because excessive cross-linking leads to degradation of transport properties. In addition to stability, we also demonstrate that our trilayer devices are able to retain data after annealing at 85 °C in 60% humidity. In order to demonstrate the retention capabilities of these devices, we performed write and erase functions on the device, annealed it at 85 °C and 60% humidity for 24 h, and measured the hysteresis. The results of this test are plotted in Fig. 3(b). It can be observed that the device remains in the low conducting state subsequent to annealing after the write step. Similarly, for the erase step, the device remains in the high conducting state after annealing. Furthermore, the hysteresis [shown in the inset of Fig. 3(b)] is preserved after performing these two tests. The improved environmental stability is attributed to the thick PS capping layer which essentially acts like a prevention barrier.

In conclusion, we describe a three layer organic memory device based on insulting polymers and C_{60} molecules. The presence of a thin layer between the Al electrode and the PVP+C_{60} nanocomposite layer is essential for repeatable device fabrication. The hysteresis in the *I-V* curves is attributed to the screening of voltage due to charging of C_{60} molecules. We demonstrate that the hysteresis can be used to perform read-write-erase functions. The hysteresis characteristics can be modified by varying the maximum positive voltage applied. This allows the control of the number of C_{60} molecules that are charged and therefore the screening voltage. This manifests itself as a variation of the discharge voltage which could be used to write multiple bits per cell. Finally, we demonstrate that just the correct amount of thermal annealing of the devices leads to enhanced stability and information retention up to 85 °C.

This research is supported by the National Science Foundation CAREER Award (ECS 0543867).

[1] R. Bez, E. Camerlenghi, A. Modelli, and A. Visconti, Proc. IEEE **91**, 489 (2003).
[2] E. Guizzo, IEEE Spectrum **41**, 17 (2004).
[3] J. C. Scott, Science **304**, 62 (2004).
[4] D. Ma, M. Aguiar, J. A. Freire, and I. A. Hummelgen, Adv. Mater. (Weinheim, Ger.) **12**, 1063 (2000).
[5] L. P. Ma, J. Liu, and Y. Yang, Appl. Phys. Lett. **80**, 2997 (2002).
[6] L. P. Ma, S. Pyo, J. Ouyang, Q. F. Xu, and Y. Yang, Appl. Phys. Lett. **82**, 1419 (2003).
[7] L. D. Bozano, B. W. Kean, V. R. Deline, J. R. Salem, and J. C. Scott, Appl. Phys. Lett. **84**, 607 (2004).
[8] J. Ouyang, C.-W. Chu, C. R. Szmanda, L. Ma, and Y. Yang, Nat. Mater. **3**, 918 (2004).
[9] T. Tsujioka and H. Kondo, Appl. Phys. Lett. **83**, 937 (2003).
[10] R. Schroeder, L. A. Majewski, and M. Grell, Adv. Mater. (Weinheim, Ger.) **16**, 633 (2004).
[11] S. Möller, C. Perlov, W. Jackson, C. Taussig, and S. R. Forrest, Nature (London) **426**, 166 (2003).
[12] A. Kanwal, S. Paul, and M. Chhowalla, Mater. Res. Soc. Symp. Proc. **830**, D7.2 (2005).
[13] S. Paul, A. Kanwal, and M. Chhowalla, Nanotechnology **17**, 145 (2006).
[14] S. R. Forrest, Nature (London) **428**, 911 (2004).
[15] G. Yu, J. Gao, J. C. Hummelen, F. Wudl, and A. J. Heeger, Science **270**, 1789 (1995).
[16] G. E. Jabbour, Y. Kawabe, S. E. Shaheen, J. F. Wang, M. M. Morrell, B. Kippelen, and N. Peyghambarian, Appl. Phys. Lett. **71**, 1762 (1997).
[17] C. D. Dimitrakopoulos, S. Purushothaman, J. Kymissis, A. Callegari, and J. M. Shaw, Science **283**, 822 (1999).
[18] G. H. Gelinck, T. C. Genus, and D. M. D. Leeuw, Appl. Phys. Lett. **77**, 1487 (2000).
[19] P. Peumans, A. Yakimov, and S. R. Forrest, J. Appl. Phys. **93**, 3693 (2003).
[20] P. K. H. Ho, J. S. Kim, I. H. Burroughes, H. Becker, S. F. Y. Li, T. M. Brown, F. Cacialli, and R. H. Friend, Nature (London) **404**, 481 (2000).
[21] H. S. Majumdar, J. K. Baral, R. Osterbacka, O. Ikkala, and H. Stubb, Org. Electron. **6**, 188 (2005).
[22] G. Teyssedre and C. Laurent, IEEE Trans. Dielectr. Electr. Insul. **12**, 857 (2005).